1990

Performance Analysis of Domestic Heat Pump Units Running on CFC Substitutes

E. C. Berlinck
Pontificia Universidade Catolica do Rio de Janeiro; Brazil

C. A. T. Uriu
Pontificia Universidade Catolica do Rio de Janeiro; Brazil

T. B. Herbas
Pontificia Universidade Catolica do Rio de Janeiro; Brazil

J. A. R. Parise
Pontificia Universidade Catolica do Rio de Janeiro; Brazil

PERFORMANCE ANALYSIS OF DOMESTIC HEAT PUMP UNITS RUNNING ON CFC SUBSTITUTES

E.C. Berlinck, C.A.T. Uriu, T.B. Herbas and J.A.R. Parise

Pontifícia Universidade Católica do Rio de Janeiro

Department of Mechanical Engineering

22453 - Rio de Janeiro - Brazil

ABSTRACT

A comparative analysis is made on the thermodynamic performance of a domestic heat pump running on CFC substitutes. A simulation model was employed for the analysis. The model is capable of predicting the operating point of the system (including condensing and evaporating pressures) as a function of equipment characteristics (for example, compressor swept volume, speed and clearance ratio, and heat exchangers overall conductances) and prevailing thermodynamic conditions (such as heat source and heat sink temperatures with the mass flow rates of their fluids). The predicted performances were compared to those of an equivalent R-12 unit, showing good agreement. Two alternative refrigerants were studied: R-134a and an azeotropic mixture of R-12 (87% in weight) and dimethylether (13%).

INTRODUCTION

A considerable amount of work has been under way in order to find available alternatives to CFC's. It is a very difficult and time-consuming task as CFC's have found a vast number of applications in today's world. In particular, domestic refrigerators and heat pumps have been using Refrigerant 12 (CCl_2F_2) for decades. Production and use of R-12, which possesses a high ozone depletion potential, is to face severe reduction following the Montreal Protocol [1]. Alternative refrigerants already exist and fall into two groups: i) substances which pose no ozone damage potential (ODP = 0); and, ii) substances that, although with chlorine, present an ODP considerable lower than that of R-12. Fluids in this second group are regarded as "temporary" CFC substitutes. Whatever the R-12 substitute, for short or long term, it will have to present most of the desired characteristics of R-12 [2,3].

The purpose of the present work is to present a comparative analysis of the performance of a small vapour-compression unit, originally designed to operate with R-12, running with CFC substitutes. Two fluids, each belonging to one of the groups discussed above, were chosen for the comparison: R-134a (1,1,1,2 - tetrafluorethane), for being considered the most promising substitute for R-12, and an azeotropic 87-13 mixture of R-12 (87% in weight) and DME (dimethylether).

For the comparative analysis a simulation model was used. The model is capable of predicting the operating point of the system as a function of equipment characteristics (heat exchangers overall conductances and compressor swept volume, rotational speed and clearance ratio) and prevailing thermodynamic conditions (such as heat source and heat sink temperatures with the mass flow rates of the fluids). One important point of study, when comparing the behaviour of different working fluids on the same equipment, is the pressure levels that are to be achieved under the operating conditions. The model, in fact, predicts the evaporating and condensing pressures, thus allowing for a more realistic analysis. A brief description of the model is presented before the performance results of the three working fluids are discussed.

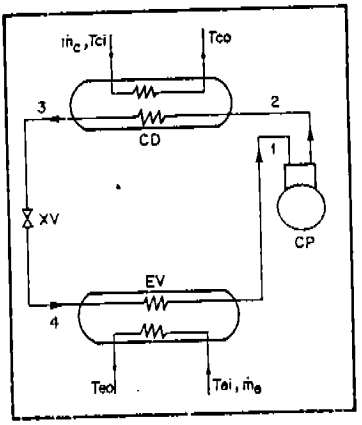

Figure 1 - Vapour compression heat pump.

THE SIMULATION MODEL

This section presents a simulation model for the steady-state operation of a basic vapour-compression cycle. The model follows closely that presented by Parise [4], although two major improvements have been included. First, condenser losses to ambient air have been taken into account. This improved considerably the agreement between predicted results and experimental data. Second, a more refined numerical method of solution has been utilized.

Compressor – For modelling the compressor, it is assumed that compression follows a polytropic process of constant index, n. With suction and discharge pressures and refrigerant inlet temperature, the state of refrigerant at the discharge plenum can be obtained.

$$v_2 = \left\{\frac{P_1}{P_2}\right\}^{1/n} v_1 \tag{1}$$

The refrigerant mass flow rate, $\dot{m}_f$, is obtained from,

$$\dot{m}_f = \frac{V_s}{v_1}\frac{w}{2\pi}\eta_v \tag{2}$$

where the volumetric efficiency, η_v, is given by,

$$\eta_v = \left\{1 + r\left[1 - \left(\frac{P_2}{P_1}\right)^{1/n}\right]\right\} C_v \tag{3}$$

C_v is an empirical volumetric coefficient which multiplies the volumetric efficiency due to the clearance volume effect, r, only.

Condenser – The condenser is treated as having a constant overall heat transfer coefficient, U_{cd}, based on maximum temperature difference. Concerning the cooling medium, the approaching temperature, mass flow rate, and specific heat are regarded as known quantities. Of course, the value of U_{cd} must take into account the desuperheating region in the condenser. The overall loss conductance, $(UA)_l$, is also known. Heat losses are supposed to occur between refrigerant and ambient only. This is typical of water cooled condensers, when refrigerant flows in the shell side. The refrigerant-to-cooling medium heat transfer process in the condenser is governed by six equations, involving the heat balances over both refrigerant and cooling medium streams, eqns. (4) and (5), the refrigerant heat break-down between

losses and cooling fluid, eqn. (6), the heat transfer equation between refrigerant and ambient, eqn. (7), and the refrigerant-to-fluid heat transfer equation, eqn. (8), using the effectiveness method.

$$\dot{Q}_f = \dot{m}_f\ (h_2 - h_3) \tag{4}$$

$$\dot{Q}_{cd} = \dot{m}_a c_{pa}(T_{co} - T_{ci}) \tag{5}$$

$$\dot{Q}_f = \dot{Q}_{cd} + \dot{Q}_l \tag{6}$$

$$\dot{Q}_l = (UA)_l \left(\frac{T_2 + T_{cd}}{2} - T_{\infty}\right) \tag{7}$$

$$\dot{Q}_{cd} = \dot{m}_a c_{pa} \epsilon_{cd}(T_2 - T_{ci}) \tag{8}$$

$$\epsilon_{cd} = 1 - exp\left[-\frac{(UA)_{cd}}{\dot{m}_a c_{pa}}\right] \tag{9}$$

Expansion valve – The present analysis concentrates on thermostatic expansion valve. It is responsible for the maintenance of a constant superheat at the compressor inlet. For the purpose of the present analysis, it has been decided to let the evaporator superheat, ΔT_s, become an input for the model. By not modelling the valve itself, one avoids the necessity of specifying valve characteristics such as flow area and discharge coefficient. Therefore,

$$T_1 = T_{ev} + \Delta T_s \tag{10}$$

Without work done or heat transfer, the enthalpy of the refrigerant remains constant.

$$h_3 = h_4 \tag{11}$$

Evaporator – The evaporator follows the condenser model in the assumption of an overall heat transfer coefficient, U_{ev}, for both the two-phase and superheated regions. Again, approaching conditions of the heat source are known, as well as the as the heat transfer area A_{ev}. In this case no heat loss, or gain, from ambient is considered. Therefore, the evaporator equations are as follows,

$$\dot{Q}_{ev} = \dot{m}_f \{(1 - x_4)h_{lve} + [h_1 - h_v(T_{ev})]\} \tag{12}$$

$$\dot{Q}_{ev} = \dot{m}_a c_{pa}(T_{ai} - T_{ao}) \tag{13}$$

$$\dot{Q}_{ev} = \dot{m}_f c_{pa} \epsilon_{ev}(T_{ai} - T_{ev}) \tag{14}$$

$$\epsilon_{ev} = 1 - exp\left[-\frac{(UA)_{ev}}{\dot{m}_a c_{pa}}\right] \tag{15}$$

Overall energy balance – An overall energy balance over the entire system gives,

$$\dot{m}_f(h_2 - h_1) + \dot{Q}_{ev} = \dot{Q}_f \tag{16}$$

Refrigerant property equations – Equations for Refrigerant-12 thermophysical properties are obtained from Gatecliff and Lady [5], equations (17) to (20), and Downing [6], (21) to (27). For Refrigerant-134a equations have been provided by Wilson and Basu [7]. Regarding the R-12/DME mixture, equations, based on an ideal mixture approach, (Apendix I), provide the property values that are compared with data from Bohnenn et al [8]. In general, the required property equations can be established as follows.

$$v_2 = v_v(T_2, P_{cd}) \ , \ v_1 = v_v(T_1, P_{ev}) \tag{17,18}$$

$$h_2 = h_v(T_2, P_{cd}) \ , \ h_1 = h_v(T_1, P_{ev}) \tag{19,20}$$

$$h_{lvc} = h_{lv}(T_{cd}) \ , \ h_{lve} = h_{lv}(T_{ev}) \tag{21,22}$$

$$h_4 = h_{4l} + x_4 h_{lve} \tag{23}$$

$$h_{4l} = h_v(T_{ev}, P_{ev}) - h_{lve} = h_l(T_{ev}) \tag{24}$$

$$h_3 = h_v(T_3, P_{sat}(T_3)) - h_{lv}(T_3) = h_l(T_3) \tag{25}$$

$$P_{ev} = P_{sat}(T_{ev}) \ , \ P_{cd} = P_{sat}(T_{cd}) \tag{26,27}$$

System of equations – A system of 27 equations have thus been formed. The equivalent twenty seven unknowns have been chosen as follows.

Compressor : $P_{cd}, P_{ev}, \eta_v, v_1, v_2, T_1, T_2, \dot{m}_f, h_1, h_2$

Condenser : $\dot{Q}_{cd}, T_{co}, h_{lvc}, T_3, \epsilon_{cd}, T_{cd}, \dot{Q}_e, \dot{Q}_f$

Expansion valve : h_3, h_4, h_{4l}

Evaporator : $\dot{Q}_{ev}, T_{eq}, h_{lve}, x_4, \epsilon_{ev}, T_{ev}$

Input data – The following parameters form the set of input data required by the model:

Compressor : V_c, r, n, w, C_v ; Condenser : T_{ci}, $\dot{m}_c$, c_{pc}, A_{cd}, U_{cd}

Expansion valve : ΔT_s ; Evaporator : T_{ei}, $\dot{m}_e$, c_{pe}, A_{ev}, U_{ev}

Any fluid can be used for the heating and cooling media, provided is heat capacity is known. In the condenser or evaporator, if only the value of UA is known, which is the most common situation with experimental data, its value can be allocated to U, and A becomes equal to unit. This is possible as U and A never appear separated in the calculations.

Solution - The system of equations (1) to (27) can be reduced, by direct substitution, to three non-linear equations, with T_2 , T_{ev} and T_{cd} as the basic variables. Schematically,

$$F_1(T_{cd}, T_{ev}, T_2) = 0 \tag{28a}$$

$$F_2(T_{cd}, T_{ev}, T_2) = 0 \tag{28b}$$

$$F_3(T_{cd}, T_{ev}, T_2) = 0 \tag{28c}$$

The system is solved numerically by the Newton-Raphson method. Then, the remaining 24 variables can be expressed in terms of T_2, T_{ev} and T_{cd}.

Comparison with experimental results - To validate a model it is important to predict accurately the performance of existing equipment. In the present work results from a water-to-water heat pump have been utilized. Experimental and predicted values were compared for a number of operating conditions. Compressor speed, evaporating and condensing pressures were the varying parameters. Details of the experimental apparatus are given by Parise [9]. For each run, the operating conditions (compressor speed, condenser and evaporator water flow rates and temperatures) and the empirical parameters (compressor volumetric coefficient, polytropic index of compression, overall efficiency and condenser and evaporator overall conductances) were entered as input data. The geometric characteristics

of components (compressor displaced volume and clearance ratio, condenser, and evaporator heat transfer areas) were also known.

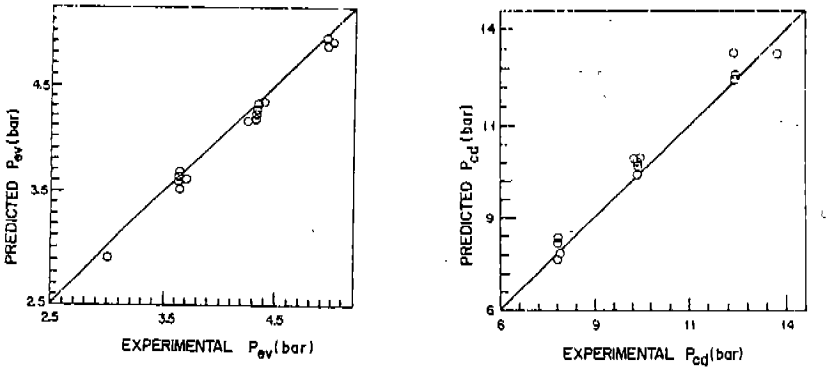

Figure 2 - Comparison between predicted and experimental values for evaporating and condensing pressures (bar).

Figure 2 shows the comparison between the experimental and predicted values for the evaporating and condensing pressures. In general a good agreement was obtained. It compares well with the overall discrepancy of 10% of reference [4], for the same experimental data. The inclusion of condenser losses certainly accounts for such an improvement. However, it should be mentioned that the model relies heavily on empirically determined coefficients ($C_v, n, U_{cd}, U_{ev.}, U_l$). When not available their estimate will certainly introduce uncertanties in the predicted results.

COMPARATIVE ANALYSIS

The model was applied for the simulation of a small heat pump unit. Input data for the model was the same for all three working fluids, as the idea was to assess the behaviour of such unit, originally designed for R-12, running with the other two substitutes. The unit chosen was of the air-water type, ie, the condenser was water cooled and the evaporator heated by air. The expansion valve was of the thermostatic type. Geometric and operational data for the heat pump model was as follows:

Compressor

eletric motor efficiency:	0.85
swept volume:	7.16 cm^3
clearance volume ratio:	0.03
polytropic index of compression:	1.19
volumetric coefficient:	0.75
compressor mechanical efficiency:	0.80
rotational speed:	3500 rpm

Condenser		Evaporator	
water inlet temperature:	35°C	air inlet temperature:	20°C
water mass flow rate:	0.015 kg/s	air mass flow rate:	0.08 kg/s
overall conductance:	250 W/°C	overall conductance:	100 W/°C
		superheat:	10°C

Some of these parameters were made to vary for the comparative analysis. The polytropic index of compression was supposed to be the same for the three working fluids. The value of 1.19 was based on past experience with different heat pumps running on R-12. Experimental data on the other two fluids is scarce. However, Kern and Wallner [10] showed that the insentropic index of R-134a remains close to that of R-12, indicating that the same would apply for the polytropic index, particularly when the same compressor is used. As for the R-12/DME mixture, the assumption of equal values for n was based on the similarity with R-12 of the thermodynamic properties. Furthermore, a value of 1.15 is given in [11] for the specific heat ratio, c_p/c_v, at 1 bar and 25°C.

The effects of the reigning conditions on both heat source and heat sink on the temperature levels of the system are presented in Figures 3 and 4. Fluid inlet temperatures and mass flow rates were varied. In Figure 3 the expected trend, of condesing and evaporating temperatures increasing with those of the heat source, T_{ei}, and heat sink, T_{ci}, has been observed. The compressor discharge temperature, T_2, follows the saturation temperature at the condenser, with the superheat (given that n is the same for all three working fluids) being determined by the equation of state. It can be seen that, for a given set of T_{ci} and T_{ei}, refrigerant 134a presented the highest temperature lift, whilst the R-12/DME mixture remained close to the R-12 curve.

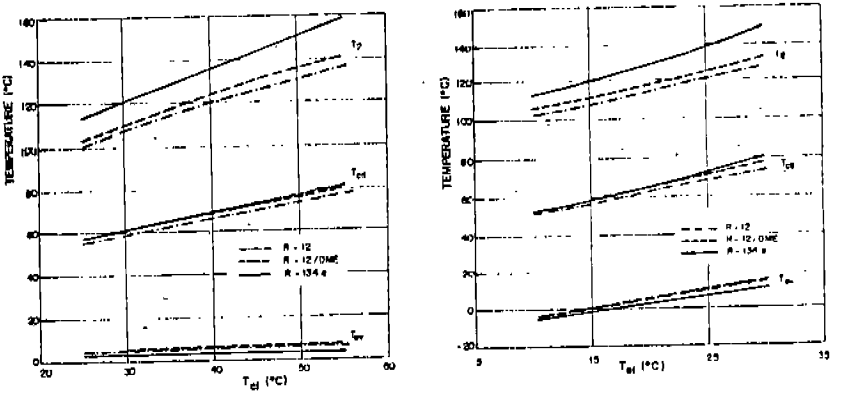

Figure 3 - Temperature levels against fluid inlet temperatures of the heat sink and heat source.

In heat pumps the temperature levels are expected to be higher than those of refrigeration units. Under these circumstances the vapour at the compressor discharge, which is at the highest temperature in the cycle, can surpass the refrigerant temperature limit, above which it becomes unstable. The consequences of refrigerant break down are discussed by Reay and Mac Michael [12]. Figure 3 shows that discharge temperatures for R-134a about 10 - 20°C above that of R-12, are to be expected. On the other hand, eventhough the condensing temperature of the R-12/DME mixture remained below that of pure R-12, its discharge temperature was slightly higher. However, more important than just a comparison with R-12 would be to assess how the predicted values of T_2 for the new refrigerants would stand against their own thermal limits. To the authors knowledge values for these limits are not available. Yet, this is an important point to be considered in the practical design of heat pumps. The same conclusions apply for Figure 4, where the fluid mass flow rates were the controlling variables.

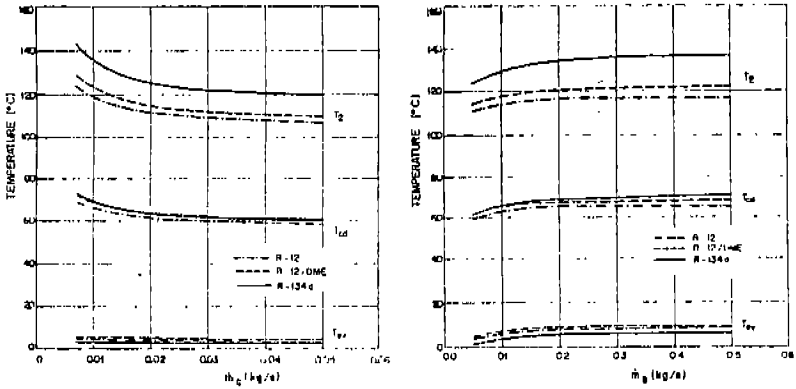

Figure 4 - Temperature levels against fluid mass flow rates of the heat sink and heat source.

To evaluate the energy consumption and cycle efficiency, the predicted values of the compressor power consumption, $\dot{W}_{cp}$, and the heating coefficient of performance, COP_h, were plotted against the condenser water and evaporator air inlet temperatures. One observes, in Figure 5, that R-12 still presents the lowest energy consumption, followed closely by R-134a. This position can be explained by a combination of the existing pressure ratio, (and, consequently, compressor volumetric efficiency), the resulting refrigerant mass flow rate and its specific volume. Surprisingly, when attention is focused on the COP_h, R-134a shows a better performance than R-12. Kuijpers et al [3] came to a different conclusion, stating that the efficiency for R-134a would be slightly lower (1%) or much lower (20%), depending on the sources of refrigerant enthalpy data. However, only an estimation formula was used [13], in opposition to the simulation model of the present work.

Concerning the R-12/DME mixture, a higher energy consumption from the compressor was observed. This, of course, affected adversely the heating coefficient of performance. Considering that the pressure ratio is similar for both R-12 and R12/DME, one could attribute such an increase to the specific volume of the vapour, which is about 20% greater for the mixture [8]. Yet, the results presented in Figure 5 are in clear disagreement with those produced by Bohnenn et al [8]. This emphasizes the necessity for further investigation.

CONCLUSION

The development of a simulation model for the performance prediction of vapour compression heat pumps has been presented. The model follows an algorithm, by which, given heat pump characteristcs and operating conditions, the heat pump steady-state performance is determined. The model here presented is basically an evolution of a previous one [4], to which condenser losses and an improved numerical method of solution were included. These modifications resulted in better agreement with experimental data. The model was employed to predict the performance of a small heat pump unit, running on three different refrigerants.

Previous predictions of CFC substitutes generally relied on the analysis of the $P \times h$ diagram, with prescribed evaporating and condensing temperatures. In practice these temperatures depend on the properties the refrigerant. Consequently, the same equipment, under the same operating conditions, would present different temperature levels. The present model was able to predict such difference, thus providing a more realistic analysis. Two substitutes were studied: R-134a and a mixture of R-12 and DME. In general R-134a presented greater

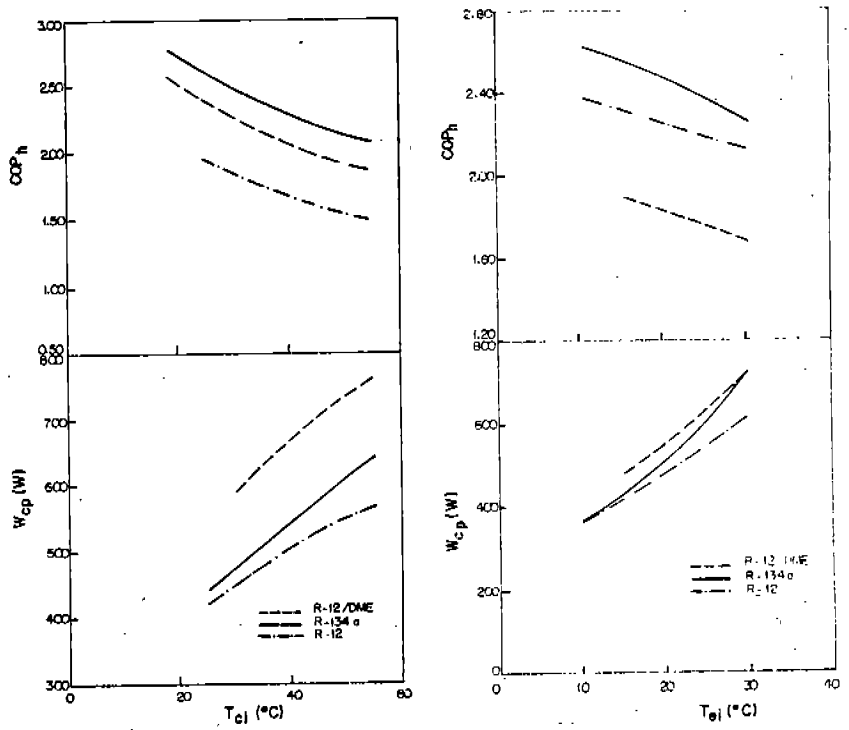

Figure 5 - Heating coefficient of performance and compressor power consumption against condenser water and evaporator air inlet temperatures.

temperature lifts. Discharge temperatures and compressor consumption were, as also predicted by other authors, higher than those for R-12. In spite of that a greater coefficient of performance was obtained for R-134a, , indicating a good heating capacity of the refrigerant. As for the R-12/DME mixture the predicted temperatures remained very close to the pure R-12 cycle. However, an increase in energy consumption was detected, with a consequent reduction on the COP_h. Since these results are in conflict with experimental data presented in a previous work [8], the authors believe that further investigation on the thermophysical properties of the mixture is required.

Finally, it should be mentioned that, in the present stage, the model did not take into account the possible alteration on the heat exchangers overall conductances due to different transport properties of the substances involved. However, it is not believed that eventual discrepancies would alter the trends presented in this work.

REFERENCES

1. Montreal Protocal on Substances thet Deplete the Ozone Layer, United Nations Environmental Programme, Final Act, 1987.
2. Dossat, R.J., Principles of Refrigeration, John Wiley & Sons Inc., 1961.
3. Kuijpers, L.J.M., de Wit, J.A. and Janssen, M.J.P., Possibilities for the replacement of CFC 12 in domestic equipment, Int Jnl Refrigeration, 11, 284-291, July 1988.
4. Parise, J.A.R., Simulation of vapour-compression heat pumps, Simulation, 46:2, pp. 71-76, 1986.
5. Gatecliff, F.W. & Lady, E.R., Explicit representation of the thermodynamic properties of refrigerants 12 and 22 in the superheat region, Purdue Comp Tech Conf, 187-190, 1974.
6. Downing, R.C., Refrigerant Equations, ASHRAE Trans, 80:2, 158-169, 1974.
7. Wilson, D.P. and Basu, R.S., Thermodynamic properties of a new stratospherically safe working fluid - refrigerant 134a, ASHRAE Trans, 94:2, paper OT-88-20-4, 1988.
8. Bohnenn, L.J.M., Vermeulen, P.E.J. and Warnaar, F.M., Introduction to the development programme of an azeotropic refrigerant mixture of CFC 12 and dimethylether, Int Jnl Ref, 11, 269-275, July 1988.
9. Parise, J.A.R., Theoretical and experimental analysis of a diesel engine driven heat pump., Ph.D. Thesis, UMIST, England, January 1983.
10. Kern, J. and Wallner, R., Impact of the Montreal Protocol on automotive air conditioning, Int Jnl Refrigeration, 11, 203-210, July 1988.
11. AKZO Chemicals Inc, preliminary data sheet, Demeon 13/87, 1988.
12. Reay, D.A. and Macmichael, D.B.A., Heat pumps, Pergamon Press, 1979.
13. Alefeld, G. Effeciency of compressor heat pumps and refrigerators derived from the Second Law of Thermodynamics, Int Jnl Refrigeration, 10, 331-341, 1988.
14. Reid, R.C., Prausnitz, J.M. and Sherwood, T.K., The properties of gases and liquids, 3rd edition, McGraw Hill, 1977.
15. Daubert, T.E., Chemical Engineering Thermodynamics, Mc Graw Hill, 1987.

APPENDIX. DERIVED THERMODYNAMIC PROPERTIES FOR THE R-12/DME MIXTURE

It is assumed that the R-12/DME mixture behaves as an ideal solution. Therefore, any given property of the mixture is related to the properties Φ of pure R-12 and DME by,

$$\Phi = 0.13\ \Phi_{DME} + 0.87\ \Phi_{R-12} \tag{A1}$$

As mentioned before, properties for R-12 were taken from [5] and [6]. Below, the equations for pure dimetylether are presented.

A1. Equation of State

The Redlich - Kwong-Soave equation [14], modified by Daubert [15], was utilized:

$$P = \frac{R-T}{V-b} - \frac{a\alpha}{T^{0.5}V(V+b)} \tag{A2}$$

$$a = \frac{\Omega_a\ R^2 T_c^{2.5}}{P_c}\ ;\ b = \frac{\Omega_b\ RT_c}{P_c} \tag{A3, A4}$$

$$\alpha = \left[1 + S\left(1 - \sqrt{\frac{T}{T_c}}\right)\right]^2 \tag{A5}$$

$$S = 0.48508 + 1.55171w - 0.1563w^2 \tag{A6}$$

$$T_c = 400\ K\ ;\ P_c = 5.37 \times 10^6\ N/m^2$$

$$\omega = 0.192 \; ; \; \Omega_a = 0.42748023 \; ; \; \Omega_b = 0.08664035$$

The molal volume of DME results from the numerical solution of equation (A2).

A2. Latent Heat of Vaporization

The DME latent heat of vaporization DME is obtained from the following equation [14],

$$\frac{h_{lv\,DME}}{RT_c} = A_1 \left(1 - \frac{T}{T_c}\right)^{0.354} + A_2 w \left(1 - \frac{T}{T_c}\right)^{0.456} \qquad (A7)$$

$$A_1 = 7.08 \; ; \; A_2 = 10.95$$

A3. Specific Enthalpy of Vapour

The enthalpy departure function [14] can be given by,

$$h_o - h_{lv} = RT(Z-1) + \left[\alpha \frac{a}{b}\left(S\sqrt{\frac{T}{T_c}\frac{1}{\alpha}} - 1\right) \; ln\left(1 + \frac{bP}{RTZ}\right)\right] \qquad (A8)$$

With the compressibility factor, Z, expressed in terms of the following cubic equation,

$$Z^3 - Z^2 + (A - B - B^2)Z - (AB) = 0 \qquad (A9)$$

$$A = \frac{\alpha\, a\, P}{R^2T^2} \; ; \; B = \frac{bP}{TT} \qquad (A10, A11)$$

The ideal gas enthalpy, h_o, is given by,

$$h_o = C_o + C_1(T - T_r) + \frac{C_2}{2}(T^2 - T_r^2) + \frac{C_3}{3}(T^3 - T_r^3) + \frac{C_4}{4}(T^4 - T_r^4) \qquad (A12)$$

$$C_0 = 4.7693 \times 10^5 \; ; \; C_1 = 3.6917 \times 10^2 \; ; \; C_2 = 3.8852$$

$$C_3 = 1.1355 \times 10^{-3} \; ; \; C_4 = 4.1605 \times^{-8} \; ; \; T_r = 233.15K$$

A5. Liquid Properties and Saturation Pressure

A constant value, $\rho_l = 1144 \; kg/_{m^3}$, was assumed for the liquid density. Following observation from Bohnenn et al [8] that the mixture vapour pressure curve is only slightly above that of R-12, the same equation [6] was employed. Assuming that the specific enthalpy of liquid (saturated or subcooled) is a function of temperature only, they, h_l can be given by,

$$h_l = h_v(T, P_{sat}(T)) - h_{lv}(T) \qquad (A13)$$

A6. Comparison of Derived Values with Available Data

Values obtained with the use of the above equations were compared with available data on the R-12/DME mixture [8]. Tipically, discrepancies of 2.3%, 12% and 0.3% were found for the prediction of and v, h_v and h_{lv}.